J. Plasma Phys. (2026), *vol*. 92, E63 © The Author(s), 2026. Published by Cambridge University Press.
This is an Open Access article, distributed under the terms of the Creative Commons Attribution licence (https://creativecommons.org/licenses/by/4.0/), which permits unrestricted re-use, distribution and reproduction, provided the original article is properly cited. doi:10.1017/S002237782610172X

Evolution of the entropy across a collisionless shock

Michael Gedalin[1] **and Vadim Roytershteyn**[2,†]

[1]Department of Physics, Ben-Gurion University of the Negev, Beer-Sheva, Israel
[2]Space Science Institute, Boulder, CO, USA

Corresponding author: Michael Gedalin, gedalin@bgu.ac.il

(Received 22 February 2026; revision received 22 February 2026; accepted 16 April 2026)

A magnetohydrodynamic (MHD) shock is a discontinuity through which plasma flows, while the mass, momentum and energy are conserved, and the entropy increases. In a collisionless system, the entropy is strictly constant along the phase-space trajectory. The MHD required entropy increase is attributed to dissipative processes causing relaxation to local thermodynamic equilibrium. The search for such dissipative processes in the shock observations usually explores variations of the entropy density or entropy per particle across the shock front. We show that both quantities may increase or decrease across the shock front even when the entropy is strictly conserved. Entropy production should be assessed using the entropy flux density.

Key words: space plasma physics, plasma nonlinear phenomena

1. Introduction

A shock is a hydrodynamic concept (see, e.g. Landau & Lifshitz 1987). A shock in plasma is a concept of magnetohydrodynamics (MHD) (de Hoffmann & Teller 1950). In both cases, a shock is a discontinuity through which a fluid flows, from upstream to downstream, and at which the density increases and the velocity decreases. The mass, momentum and energy are conserved, and at an MHD shock, the tangential component of the electric field is continuous. These conservation laws are used to establish the relation between the upstream and downstream parameters. It is also required that the entropy of the fluid (plasma in what follows) at the downstream side be higher than the entropy at the upstream side, in accordance with the second law of thermodynamics (Landau & Lifshitz 1987). Real shocks are transition layers of finite width. In a collision-dominated plasma, where the binary Coulomb collisions play an important role, the width is determined by the dissipative processes related to collisions. In a collisionless plasma, the behaviour of the plasma within the transition layer is determined by the electromagnetic fields generated self-consistently by the plasma species. The MHD requirement of the entropy increase

[†]Present address: Los Alamos National Laboratory, Los Alamos, NM 87545, USA.

is valid both for collisional and collisionless plasmas, and is generally thought to be related to dissipative processes. The search for such dissipative processes remains one of the central problems of collisionless shock physics.

Modern high-resolution measurements at the Earth's bow shock allow in-depth, detailed studies of the behaviour of particle distributions across the shock (Schwartz *et al*. 2022; Agapitov *et al*. 2023). Analysis of the entropy production within the shock requires the usage of the appropriate quantity (Parks *et al*. 2012; Liang *et al*. 2019; Du *et al*. 2020). Typically, the entropy density or the entropy per particle (see below) is used, and an increase of the parameter is interpreted as a result of some dissipative process occurring in the shock. Here, we show that, in a collisionless shock, the entropy flux density is conserved, while the entropy density and the entropy per particle may change either way upon shock crossing. Accordingly, any conclusion about entropy production should be made on the basis of the measurements of the variation of the entropy flux density across the shock.

2. Entropy in non-equilibrium open systems with flows

The standard definitions of entropy in statistical mechanics, such as $\ln \Gamma$ in an isolated system, where Γ is the number of available microscopic states, or as the sum over all available microscopic states $-\sum_a p_a \ln p_a$, where p_a is the probability of the microscopic state a, are applicable in the standard static statistical ensembles (Reichl 2009). The extension of the definition of entropy in non-equilibrium open systems with flows should be consistent with the standard definitions. For completeness, we briefly outline here the procedure of such an extension. Consider an ideal gas in a thermodynamic equilibrium. The entropy per particle is (Reichl 2009)

$$\sigma = \frac{5}{2} - \ln\left(n\lambda_T^3\right), \tag{2.1}$$

$$n = \frac{N}{V}, \quad \lambda_T = \frac{h}{\sqrt{2\pi m T}}, \tag{2.2}$$

where N is the number of particle, V is the volume, h is the Planck constant, m is the particle mass, T is the temperature and n is the number density. Let

$$\mathcal{P} = \frac{N\exp\left(-p^2/2mT\right)}{\int \exp(-p^2/2mT)\mathrm{d}^3\boldsymbol{r}\mathrm{d}^3\boldsymbol{p}/h^3} = n\lambda_T^3 \exp\left(-\frac{p^2}{2mT}\right), \tag{2.3}$$

where we used $\int \mathrm{d}^3\boldsymbol{r} = N$. Note that

$$\int \mathcal{P}\mathrm{d}^3\boldsymbol{p} = nh^3. \tag{2.4}$$

Consider now the expression

$$s = -\int \mathcal{P}(\ln\mathcal{P} - 1)\frac{\mathrm{d}^3\boldsymbol{p}}{h^3} \tag{2.5}$$

$$= -\int \mathcal{P}\left(-\frac{p^2}{2mT} + \ln\left(n\lambda_T^3\right) - 1\right)\frac{\mathrm{d}^3\boldsymbol{p}}{h^3} \tag{2.6}$$

$$= \frac{5}{2}n - n\ln\left(n\lambda_T^3\right) = n\sigma, \tag{2.7}$$

https://doi.org/10.1017/S002237782610172X Published online by Cambridge University Press

which is the entropy density and $w = -\mathcal{P}(\ln \mathcal{P} - 1)/h^3$ is the phase-space entropy density.

Let now $f(\boldsymbol{r}, \boldsymbol{p}, t)$ be a single-particle distribution function such that

$$\int f(\boldsymbol{r}, \boldsymbol{p}, t)\mathrm{d}^3\boldsymbol{p} = n(\boldsymbol{r}, t). \tag{2.8}$$

The distribution function $f(\boldsymbol{r}, \boldsymbol{p}, t)$ is the generalisation of the equilibrium $\mathcal{P}(\boldsymbol{p})$.

Then the phase-space entropy density w and the entropy density s in a non-equilibrium system, described by a single-particle distribution function f, can be defined as follows:

$$w = -f(\ln(h^3 f) - 1), \tag{2.9}$$

$$s(\boldsymbol{r}, t) = -\int f(\ln(h^3 f) - 1)\mathrm{d}^3\boldsymbol{p} = -\int f \ln(h^3 f)\mathrm{d}^3\boldsymbol{p} + n(\boldsymbol{r}, t). \tag{2.10}$$

Accordingly, the entropy per particle would be

$$\sigma(\boldsymbol{r}, t) = 1 - \frac{1}{n}\int f \ln(h^3 f)\mathrm{d}^3\boldsymbol{p}. \tag{2.11}$$

These expressions are more precise definitions of the usually used Boltzmann entropy (Parks *et al*. 2012; Liang *et al*. 2019; Du *et al*. 2020; Agapitov *et al*. 2023). The total entropy within a certain volume is

$$S = \int s\mathrm{d}^3\boldsymbol{r} = \int n\sigma\mathrm{d}^3\boldsymbol{r}. \tag{2.12}$$

3. Conservation of Boltzmann entropy

The collisionless Vlasov equation is

$$\frac{\partial f}{\partial t} + \boldsymbol{v}\cdot\frac{\partial f}{\partial \boldsymbol{r}} + q\left(\boldsymbol{E} + \frac{1}{c}\boldsymbol{v}\times\boldsymbol{B}\right)\cdot\frac{\partial f}{\partial \boldsymbol{p}} = 0, \tag{3.1}$$

which alternatively reads

$$\frac{\mathrm{d}f}{\mathrm{d}t} = 0 \tag{3.2}$$

along the trajectory $\dot{\boldsymbol{r}} = \boldsymbol{v}$, $\dot{p} = q(\boldsymbol{E} + (1/c)\boldsymbol{v}\times\boldsymbol{B})$. For each function $F(f)$ such that $F(f = 0) = 0$ we get

$$\frac{\mathrm{d}F}{\mathrm{d}t} = \left(\frac{\mathrm{d}F}{\mathrm{d}f}\right)\left(\frac{\mathrm{d}f}{\mathrm{d}t}\right) = 0, \tag{3.3}$$

that is

$$\frac{\partial F}{\partial t} + \boldsymbol{v}\cdot\frac{\partial F}{\partial \boldsymbol{r}} + \frac{q}{m}\left(\boldsymbol{E} + \frac{1}{c}\boldsymbol{v}\times\boldsymbol{B}\right)\cdot\frac{\partial F}{\partial \boldsymbol{v}} = 0. \tag{3.4}$$

https://doi.org/10.1017/S002237782610172X Published online by Cambridge University Press

Taking the lowest moment one has

$$\frac{\partial}{\partial t}\left(\int F(f(\boldsymbol{p},\boldsymbol{r},t))\mathrm{d}^3\boldsymbol{p}\right)+\frac{\partial}{\partial \boldsymbol{r}}\cdot\left(\int \boldsymbol{v}F(f(\boldsymbol{p},\boldsymbol{r},t))\mathrm{d}^3\boldsymbol{p}\right)=0. \tag{3.5}$$

In the stationary one-dimensional case, where everything depends only on the x-coordinate, one has

$$\int v_x F(f(\boldsymbol{p},x))\mathrm{d}^3\boldsymbol{p}=\text{const}. \tag{3.6}$$

In particular, if $F=-f(\ln(h^3 f)-1)$, the corresponding moment

$$s=-\int f(\ln(h^3 f)-1)\mathrm{d}^3\boldsymbol{p} \tag{3.7}$$

is the entropy density and

$$\boldsymbol{j}_s=-\int \boldsymbol{v}f(\ln(h^3 f)-1)\mathrm{d}^3\boldsymbol{p} \tag{3.8}$$

is the entropy flux density. Conservation of entropy means

$$\frac{\partial s}{\partial t}+\nabla\cdot\boldsymbol{j}=0. \tag{3.9}$$

Entropy production would mean the appearance of a positive source term on the right-hand side of (3.9)

$$\frac{\partial s}{\partial t}+\nabla\cdot\boldsymbol{j}=\left(\frac{\mathrm{d}s}{\mathrm{d}t}\right)_{source} \tag{3.10}$$

with $(\mathrm{d}s/\mathrm{d}t)_{source}>0$, as required by the second law of thermodynamics. If the shock is one-dimensional and stationary, $(\partial/\partial t)=0$ and $(\partial/\partial y)=(\partial/\partial z)=0$, then (3.9) means $j_{s,x}=\text{const}$, in the absence of entropy production. The entropy flux density is constant throughout.

Let $(\boldsymbol{r},\boldsymbol{p},t)$ be a solution of the equations of motion

$$\frac{\mathrm{d}\boldsymbol{r}}{\mathrm{d}t}=\boldsymbol{v},\qquad \frac{\mathrm{d}\boldsymbol{p}}{\mathrm{d}t}=q\left(\boldsymbol{E}+\frac{1}{c}\boldsymbol{v}\times\boldsymbol{B}\right) \tag{3.11}$$

with the initial conditions $(\boldsymbol{r}_0,\boldsymbol{p}_0,t_0)$. For a one-dimensional time-independent shock $f(\boldsymbol{p},x)=f_0(\boldsymbol{p}_0,x_0)$.

Consider a thin tube of particles starting at x_0 with the velocities in the infinitesimal momentum volume $\mathrm{d}\boldsymbol{p}_0$ around $\boldsymbol{p}_0$, corresponding to $\boldsymbol{v}_0$. Let this infinitesimal region be Liouville mapped to $\mathrm{d}\boldsymbol{p}$ around $\boldsymbol{p}$, corresponding to $\boldsymbol{v}$, at x. The infinitesimal incident flux at x_0 is

$$\mathrm{d}j=v_{0x}f_0(\boldsymbol{p}_0,x_0)\mathrm{d}^3\boldsymbol{p}_0. \tag{3.12}$$

The flux conservation means that the same flux crosses x

$$v_x f(\boldsymbol{p},x)\mathrm{d}^3\boldsymbol{p}=\mathrm{d}j, \tag{3.13}$$

https://doi.org/10.1017/S002237782610172X Published online by Cambridge University Press

which gives

$$\mathrm{d}^3\boldsymbol{p} = \left|\frac{v_{0x}}{v_x}\right| \mathrm{d}^3\boldsymbol{p}_0 \tag{3.14}$$

and therefore, for each function $F(f)$ one has $F(f(\boldsymbol{p}, x)) = F(f_0(\boldsymbol{p}_0, x_0))$ and

$$\int F(f(\boldsymbol{p}, x))\mathrm{d}^3\boldsymbol{p} = \int F(f_0(\boldsymbol{p}_0, x_0)) \left|\frac{v_{0x}}{v_x}\right| \mathrm{d}^3\boldsymbol{p}_0 \neq \int F(f_0(\boldsymbol{p}_0, x_0))\mathrm{d}^3\boldsymbol{p}_0. \tag{3.15}$$

The entropy conservation requires $j_x = \text{const}$ throughout In general,

$$s/n = -\left[\int f_0 \ln f_0 \left|\frac{v_{0x}}{v_x}\right| \mathrm{d}^3\boldsymbol{p}_0\right] \Big/ \left[\int f_0 \left|\frac{v_{0x}}{v_x}\right| \mathrm{d}^3\boldsymbol{p}_0\right] \tag{3.16}$$

$$\neq -\left[\int f_0 \ln f_0 \mathrm{d}^3\boldsymbol{p}_0\right] \Big/ \left[\int f_0 \mathrm{d}^3\boldsymbol{p}_0\right] = s_0/n_0 \tag{3.17}$$

and, therefore, $s_d/n_d \neq s_u/n_u$. In the above integrals $\boldsymbol{p}$ and $\boldsymbol{v}$ are functions of $\boldsymbol{p}_0$.

Often, analysis is done in dimensionless variables. The distribution function is also dimensionless then. Let the number density be normalised with n_0, and the velocity with v_0, that is,

$$n = Nn_0,\ \boldsymbol{v} = \boldsymbol{V}V_0, \tag{3.18}$$

$$N = \int F\mathrm{d}^3\boldsymbol{V}, \tag{3.19}$$

$$F = f\frac{m^3V_0^3}{n_0}. \tag{3.20}$$

Then the entropy density is

$$S = n_0 s = -\int F\left(\ln\left(\frac{n_0h^3}{m^3V_0^2}F\right)\boldsymbol{V} - 1\right)\mathrm{d}^3\boldsymbol{V} \tag{3.21}$$

$$= -\int F \ln F \mathrm{d}^3\boldsymbol{V} - N\ln\frac{n_0h^3}{em^3V_0^2}. \tag{3.22}$$

The difference of the entropy densities $S_d - S_u$ may appear positive or negative depending on the normalisation. Therefore, it is less informative than the entropy per particle

$$\frac{S}{N} = -\frac{1}{N}\int F \ln F \mathrm{d}^3\boldsymbol{V} - \ln\frac{n_0h^3}{em^3V_0^2}. \tag{3.23}$$

The second term is constant and can be safely omitted when the variations of the entropy per particle are analysed. Similarly, the entropy flux is

$$n_0\boldsymbol{j}_s = -V_0\int \boldsymbol{V}F\left(\ln\left(\frac{n_0h^3}{m^3V_0^2}F\right)\boldsymbol{V} - 1\right)\mathrm{d}^3\boldsymbol{V} \tag{3.24}$$

$$= -V_0\int F\ln F\mathrm{d}^3\boldsymbol{V} - \left(\ln\frac{n_0h^3}{em^3V_0^2}\right)N\boldsymbol{V}. \tag{3.25}$$

https://doi.org/10.1017/S002237782610172X Published online by Cambridge University Press

Thus, the normalisation adds a constant term to the entropy per particle and a term proportional to the particle flux density to the entropy flux. Note that, in a local thermodynamic equilibrium, described by the shifted Maxwellian

$$f_M = n\left(\frac{m}{2\pi T}\right)^{3/2}\exp\left(-\frac{m(\boldsymbol{v}-\boldsymbol{V})^2}{2T}\right), \tag{3.26}$$

where n, $\boldsymbol{V}$ and T depend on $\boldsymbol{r}$ and t, the entropy density and the entropy flux density are related by $\boldsymbol{j}_s = s\boldsymbol{V}$. In the general case, however, $\boldsymbol{j}_s \neq s\boldsymbol{V}$.

In the one-dimensional stationary case, the particle flux density is constant. Since we are interested in the changes across the shock front, in the subsequent numerical analysis, we address only the variable parts, that is,

$$\frac{s}{n} = -\frac{\int f\ln f\,\mathrm{d}^3\boldsymbol{v}}{\int f\,\mathrm{d}^3\boldsymbol{v}} = -\frac{\int f_0\ln f_0\,|(v_{0x}/v_x)|\,\mathrm{d}^3\boldsymbol{v}_0}{\int f_0\,|(v_{0x}/v_x)|\,\mathrm{d}^3\boldsymbol{v}_0}, \tag{3.27}$$

$$j_{sx} = -\int v_x f\ln f\,\mathrm{d}^3\boldsymbol{v} = -\int v_x f_0\ln f_0\left|\frac{v_{0x}}{v_x}\right|\mathrm{d}^3\boldsymbol{v}_0, \tag{3.28}$$

where we reversed the notation to the more convenient lower case. The normalisation here is arbitrary. Only the difference $s_d/n_d - s_u/n_u$ is meaningful. A non-zero difference $j_{sxd} - j_{sxu}$ would mean entropy production. In a collisionless shock $j_{sx} = \text{const}$ throughout the shock, so that $j_{sxd} = j_{sxu}$. The standard Rankine–Hugoniot relations assume that the upstream and downstream plasmas are in local thermodynamic equilibrium and require $s_d/n_d > s_u/n_u$ (Landau, Lifshitz & Pitaevskiĭ 1984; Landau & Lifshitz 1987).

4. An analytic example: electrostatic shock

An electrostatic shock is a one-dimensional jump in the potential, through which a plasma flows. If the potential is $\phi(x)$, the energy of a particle $\epsilon = mv^2/2 + q\phi$ is conserved in the collisionless regime. For each species $f = f(\epsilon)$. Let the upstream distribution be a one-dimensional shifted Maxwellian

$$f_0(v_0) = \exp\left(-\frac{(v_0 - V_u)^2}{2v_T^2}\right). \tag{4.1}$$

We use the freedom in normalisation to avoid keeping unnecessary constants. The energy conservation is

$$v_0 = \sqrt{v^2 + 2q\phi/m}, \tag{4.2}$$

therefore

$$f(x, v) = \exp\left(-\frac{(\sqrt{v^2 + 2q\phi/m} - V_u)^2}{2v_T^2}\right) \tag{4.3}$$

and

$$\sigma = \frac{1}{N}\int\left(\frac{(\sqrt{v^2 + 2q\phi/m} - V_u)^2}{2v_T^2}\right)\exp\left(-\frac{(\sqrt{v^2 + 2q\phi/m} - V_u)^2}{2v_T^2}\right)\mathrm{d}v \tag{4.4}$$

$$= \frac{1}{N}\int\left(\frac{((v_0 - V_u)^2}{2v_T^2}\right)\exp\left(-\frac{(v_0 - V_u)^2}{2v_T^2}\right)\frac{v_0}{v}\mathrm{d}v_0, \tag{4.5}$$

https://doi.org/10.1017/S002237782610172X Published online by Cambridge University Press

$$N = \frac{n}{n_0} = \int \exp\left(-\frac{(\sqrt{v^2 + 2q\phi/m} - V_u)^2}{2v_T^2}\right) \mathrm{d}v \tag{4.6}$$

$$= \int \exp\left(-\frac{(v_0 - V_u)^2}{2v_T^2}\right) \frac{v_0}{v} \mathrm{d}v_0. \tag{4.7}$$

If $v_T \ll V_u$ then

$$\frac{n}{n_0} \approx \frac{V_u}{\sqrt{V_u^2 - 2q\phi/m}}, \tag{4.8}$$

$$\frac{\sigma}{\sigma_0} \approx \frac{V_u}{\sqrt{V_u^2 - 2q\phi/m}}. \tag{4.9}$$

For $q\phi < 0$ one would have $\sigma < \sigma_0$.

5. Test particle analysis

The equations of motion inside the shock transition are not integrable analytically, and there is no closed analytical expression, neither for $f(\boldsymbol{p}, x)$ nor for $v_x(x, v_{0x}, x_0)$. Instead, we trace ions across a model shock front by numerically solving the ion equations of motion in prescribed stationary electric and magnetic fields. The fields depend only on the coordinate x along the shock normal. The Maxwellian distributed incident ions are traced across the shock front. There is a set of layers $x_i < x < x_i + \Delta x$, $x_i = x_l + (i-1)\Delta x$, $i = 1, \ldots, N$, for the numerical derivation of the moments of the distribution function. Each ion contributes to the moment in a layer as many times as it is found in the layer, which is $\Delta x/|v_x|$ for sufficiently narrow layers (the staying time method). Multiplying by the weight $|v_{0x}|$ accounts for the Jacobian $|v_{0x}|/|v_x|$. In the numerical calculation of the moments, the staying time method accounts for the denominator $1/|v_x|$, since each ion contributes $\Delta x/|v_x|$ times, provided Δx is sufficiently small. The incident flux is taken into account by the weight $|v_{0x}|$ assigned to each particle. The additional factor is simply

$$\ln f_0 = -\left(\frac{(v_{0x} - 1)^2 + v_{0y}^2 + v_{0z}^2}{2v_T^2}\right). \tag{5.1}$$

The focus of the study is the effect of the macroscopic stationary fields on the entropy, so that the shock model does not have to be self-consistent. We chose the model fields as follows:

$$B_z = \sin\theta_{Bn}\left(\frac{R+1}{2} + \frac{R-1}{2}\tanh\frac{3x}{D}\right), \tag{5.2}$$

$$B_y = \frac{\cos\theta_{Bn}}{M_A}\frac{\mathrm{d}B_z}{\mathrm{d}x}, \tag{5.3}$$

$$B_x = \cos\theta_{Bn}, \tag{5.4}$$

$$E_y = \sin\theta_{Bn}, \tag{5.5}$$

$$E_x = -l_E\frac{\mathrm{d}B_z}{\mathrm{d}z}, \tag{5.6}$$

$$E_z = 0. \tag{5.7}$$

https://doi.org/10.1017/S002237782610172X Published online by Cambridge University Press

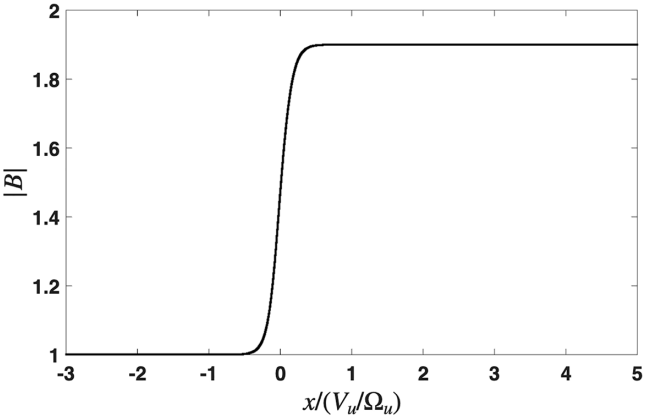


FIGURE 1. The magnitude of the model magnetic field.

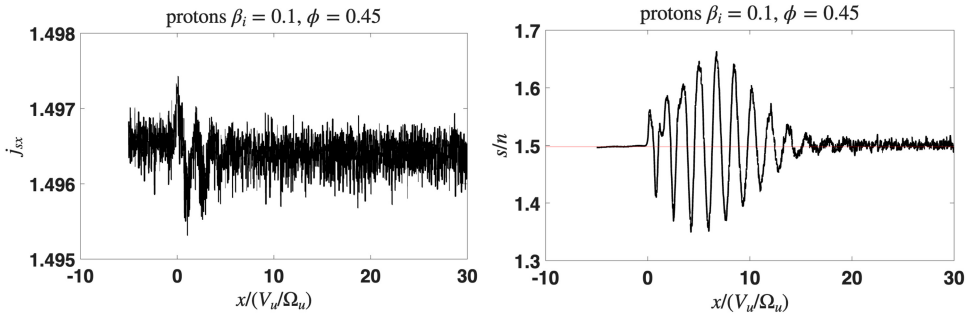


FIGURE 2. Left: the entropy flux density. Right: the entropy per particle.

Here, the magnetic field $\boldsymbol{B}$ is normalised with the upstream magnetic field B_u, the electric field $\boldsymbol{E}$ is normalised with $V_u B_u/c$ and the coordinate is normalised with the upstream convective gyroradius V_u/Ω_u, $\Omega_u = eB_u/m_p c$. The coefficient l_E is obtained from the condition $-\int E_x \, \mathrm{d}x = \phi$, where ϕ is the cross-shock potential normalised with $m_p V_u^2/2$. The parameter R is related to the magnetic compression ratio as follows:

$$\frac{B_d}{B_u} = \sqrt{R^2 \sin^2\theta_{Bn} + \cos^2\theta_{Bn}}. \tag{5.8}$$

The Alfvénic Mach number $M_A = V_u/v_A$, where $v_A = B_u/\sqrt{4\pi n_u m_p}$ is the Alfvén speed, the ramp width D, the magnetic compression ratio B_d/B_u, the shock angle θ_{Bn} and the cross-shock potential ϕ are the variable parameters of the model. In the following analysis $M_A = 2$, $B_d/B_u = 1.9$, $\theta_{Bn} = 60^\circ$ and $D = 1/M_A$. The cross-shock potential ϕ and the incident ion $\beta_i = 8\pi n_u T_u/B_u^2$ are varied. Figure 1 shows the magnitude of the model magnetic field. Figure 2 shows the entropy flux density j_{sx} and the entropy per particle s/n as a function of the coordinate along the shock normal, for $\beta_i = 0.1$ and the normalised cross-shock potential $\phi = 0.45$. The flux is conserved, as expected. The entropy per particle also remains constant, $s_d/n_d = s_u/n_u$. This may make an impression that the heating is adiabatic, in the sense that

https://doi.org/10.1017/S002237782610172X Published online by Cambridge University Press

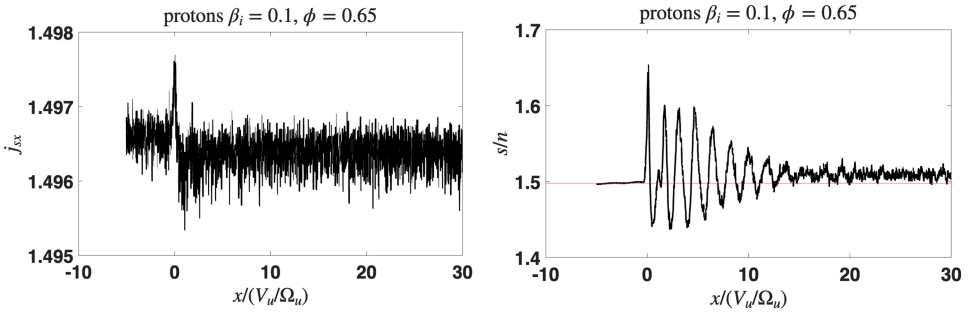


FIGURE 3. Left: the entropy flux density. Right: the entropy per particle.

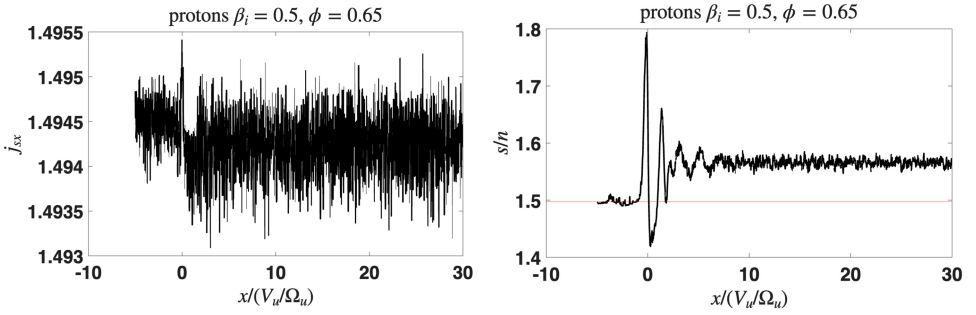


FIGURE 4. Left: the entropy flux density. Right: the entropy per particle.

$n/T^{3/2} = \text{const}$. However, adiabaticity implies thermodynamic equilibrium, while the downstream distribution is not Maxwellian. The amount of ion heating is roughly determined by $|\sqrt{1-\phi} - V_d|$. The conservation of s/n in this case is coincidental and due to the choice of the parameters.

Figure 3 shows the entropy flux density j_{sx} and the entropy density s as a function of the coordinate along the shock normal, for $\beta_i = 0.1$ and the normalised cross-shock potential $\phi = 0.65$. The entropy flux is conserved. However, $s_d/n_d > s_u/n_u$, although the difference is small. The larger cross-shock potential increases the dispersion of $|v_x|$ in the denominator of (3.27). Since the ions are decelerated at the shock crossing, this increase of the velocity dispersion causes the weak increase in s/n.

Figure 4 shows the entropy flux density j_{sx} and the entropy density s as a function of the coordinate along the shock normal, for $\beta_i = 0.5$ and the normalised cross-shock potential $\phi = 0.45$. The entropy flux is conserved. In this case, $s_d/n_d > s_u/n_u$ noticeably. This change occurs due to the larger dispersion of $|v_x|$ in the denominator of (3.27) for the higher initial thermal speed of the ions.

Figure 5 shows the results of a similar electron tracing across the same model shock. In contrast with ions, electrons are accelerated across the shock by the cross-shock potential. In addition, because of their small mass, the ratio of their upstream thermal speed to the shock speed $v_{Te}/V_u = \sqrt{m_i/m_e}\sqrt{\beta/2}/M_A$ is by the factor $\sqrt{m_i/m_e}$ larger than that of ions with the same β. To reduce computational time, the mass ratio in the electron tracing was set to $m_e/m_i = 1/100$. In figure 5 the electron $\beta = 0.05$ and $\phi = 0.45$. Figure 6 shows the results of another electron

https://doi.org/10.1017/S002237782610172X Published online by Cambridge University Press

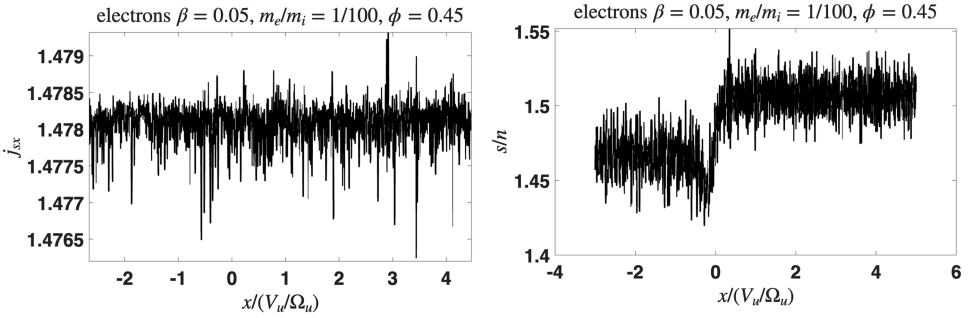


FIGURE 5. Left: the entropy flux density. Right: the entropy per particle.

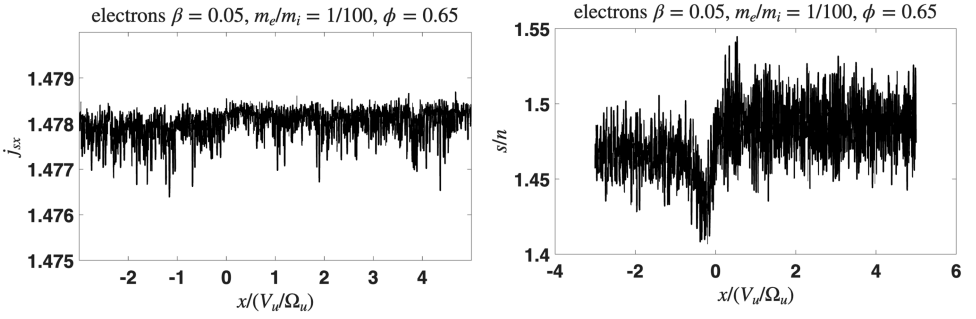


FIGURE 6. Left: the entropy flux density. Right: the entropy per particle.

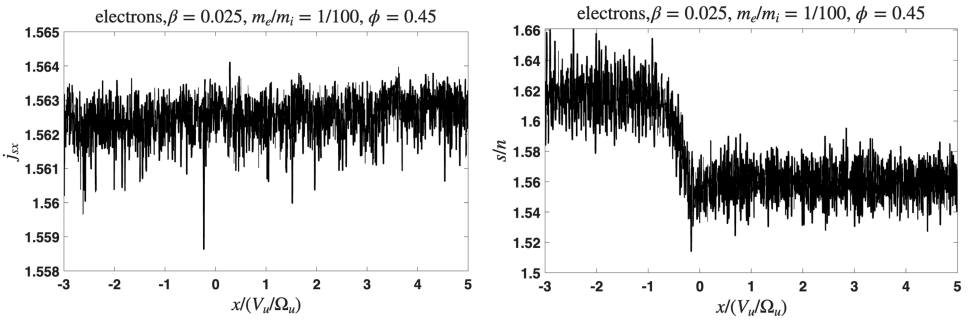


FIGURE 7. Left: the entropy flux density. Right: the entropy per particle.

tracing across the same model shock. The electron $\beta = 0.05$ and $\phi = 0.65$. Figure 7 shows the results of yet another electron tracing across the same model shock. This time the electron $\beta = 0.025$ and $\phi = 0.45$. The entropy flux is conserved, while the entropy per particle decreases. The decrease in this case is related to the acceleration of the electrons across the shock front and small dispersion of $|v_x|$ in the denominator of (3.27).

https://doi.org/10.1017/S002237782610172X Published online by Cambridge University Press

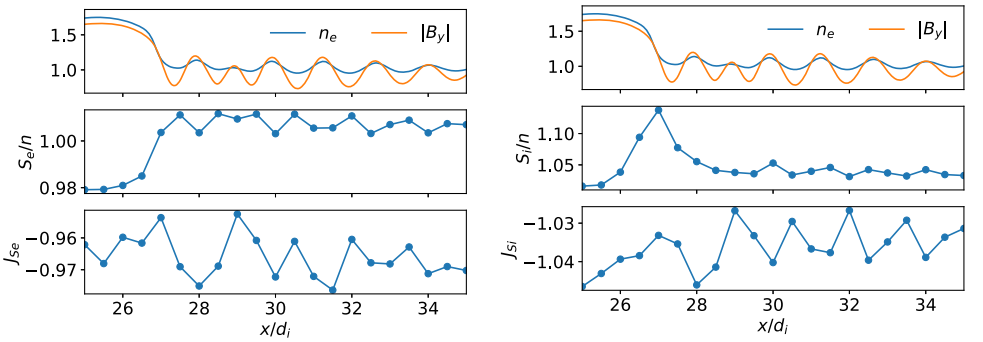


FIGURE 8. Top: the electron density and the magnetic field. Middle: the entropy per particle. Bottom: the entropy flux density. Left column: electrons. Right column: ions. Upstream is on the right, downstream is on the left.

6. Simulations

The above test particle analysis shows that entropy is strictly conserved in a time-independent planar shock. This conservation takes the form $\mathrm{d}j_{s,x}/\mathrm{d}x = 0$. On the other hand, the entropy per particle may increase or decrease, depending on the particle charge sign, cross-shock potential and the temperature of the upstream incident distribution. The test particle analysis does not take into account the field fluctuations, produced self-consistently by the charged particles. To understand the role of these fluctuations, we performed particle-in-cell (PIC) simulations.

The two-dimensional PIC simulation of a low-Mach-number shock presented here was performed using the VPIC code (Bowers *et al*. 2008). The shock is created by the reflection of plasma flowing in the negative x direction from a rigid, perfectly conducting wall. The upstream distributions for both electrons and ions are Maxwellian, with density n_0 and temperatures T_e and T_i, respectively. The angle between the upstream magnetic field B_0 and the x-axis is $\theta_{Bn} = 111°$. The upstream magnetic field is in the xy plane. The plasma is injected from the right boundary of the domain at $x = L_x$ with the inflow speed $V_{in} = 1V_A$, where $V_A = B_0/\sqrt{4\pi n_0 m_i}$ is the Alfvén speed. The shock moves in the positive x direction with the average speed $V_{sh} = 1.42V_A$, such that the upstream flow in the shock frame V_0 is characterised by the Mach number $M_A = V_0/V_A = 2.42$. The upstream $\beta_i = 0.3$ and $\beta_e = 2.6$, where $\beta_s = 8\pi n_0 T_s/B_0^2$ and $s = e, i$ denotes plasma species. The simulation domain has dimensions $L_x \times L_y = (50 \times 5)d_i$, where $d_s = c/\omega_{ps}$, c is the speed of light and $\omega_{ps} = (4\pi n_0 e^2/m_s)^{1/2}$. The domain is resolved by a uniform Cartesian grid with resolution $N_x \times N_y = 18\,816 \times 1984$ cells, such the cell size is approximately one Debye length in the upstream plasma. The mass ratio is $m_i/m_e = 1836$. The ratio between the electron plasma frequency ω_{pe} and the electron cyclotron frequency Ω_{ce} is $\omega_{pe}/\Omega_{ce} = 10$, where $\Omega_{cs} = eB_0/(m_s c)$. The simulation time step is $\delta t\omega_{pe} \approx 0.06$.

To compute the entropy, y-averaged distribution functions were accumulated on a three-dimensional velocity grid at regular intervals. The distributions were further averaged over a small interval $\delta x \approx 0.05d_i$. The velocity grid resolution was approximately $0.4V_A$ for electrons and $8.5 \times 10^{-3}V_A$ for ions. The entropy density and the entropy flux were obtained by numerical integration of the reconstructed distribution over this grid. We have verified that the results are converged with respect to the resolution of the velocity-space grid. Figure 8 shows the results for the electrons (left

https://doi.org/10.1017/S002237782610172X Published online by Cambridge University Press

column) and ions (right column) at time $t = 19\Omega_{ci}^{-1}$. The top panel shows profiles of the density and magnetic field. The middle panel is the entropy density per particle, normalised to the upstream reference value $S_{0i} = n_0[3/2 - \log n_0 + 3\log(\sqrt{\pi} v_{ts})]$, where $v_{ts}^2 = 2T_s/m_s$. Finally, the bottom panel shows the entropy flux for each species normalised to $V_0 S_{0s}$. Multiple relatively small amplitude instabilities are present in the simulation, especially in the vicinity of the ramp. The influence of these fluctuations on the evolution of entropy per particle and entropy flux density is self-consistently accounted for. There is no substantial effect of the fluctuations on the entropy flux density, so that no significant entropy production is found.

7. Discussion

The electromagnetic fields in the collisionless Vlasov equation (3.1) are completely arbitrary. They may include small-scale fast fluctuations which do not break the entropy conservation (3.9). Entropy in collisionless systems is known to be produced due to the coarse graining of the distribution when the inhomogeneity in the velocity space proceeds toward smaller and smaller scales, as occurs in the Landau damping (Mouhot & Villani 2011) and, in general, in the resonant wave–particle interactions, where the information about the wave phases is lost. This interaction adds a diffusion-type term to the kinetic equation for the coarse-grained distribution function (see, e.g. Sarazin *et al*. 2009). Non-resonant wave–particle interactions retain the phase information and cannot contribute to the coarse-grained entropy production. Thus, ion reflection cannot be a dissipative process resulting in entropy production. The test particle analysis, even with small-scale features included, cannot take into account resonant interactions. Simulations necessarily include coarse graining due to the discretisation. However, PIC simulations of a low-Mach-number shock have not revealed entropy production at a sufficiently significant level.

8. Conclusions

The entropy in a collisionless shock, which is an open collisionless system with a flow, is conserved in the absence of processes that involve phase randomisation or unless coarse graining is applied. This conservation in a stationary planar shock takes the form $j_{sx} = -\int v_x f \ln f \mathrm{d}^3\boldsymbol{v} = \text{const}$. The upstream and downstream entropy densities $s = -\int f \ln f \mathrm{d}^3\boldsymbol{v}$ and entropies per particle s/n may be different. The downstream values may be larger or smaller than the upstream values. If the upstream and downstream plasmas were in local thermodynamic equilibrium, the second law of thermodynamics would require $s_d/n_d > s_u/n_u$. In a collisionless shock, the downstream plasma may not reach thermodynamic equilibrium even well beyond the shock transition, and the above requirement does not hold. The search for irreversible processes in the observed collisionless shock front using the entropy variation across the shock should focus on the variation of the entropy flux rather than on the entropy density or entropy per particle.

Acknowledgements

Editor Antoine C. Bret thanks the referees for their advice in evaluating this article.

Funding

The work performed at SSI was supported by NSF grant 2512084. Computational resources were provided by the NASA High-End Computing (HEC) Program

https://doi.org/10.1017/S002237782610172X Published online by Cambridge University Press

through the NASA Advanced Supercomputing (NAS) Division at Ames Research Center and by Texas Advanced Computing Center (TACC) at the University of Texas at Austin. Access to TACC resources was provided by the Frontera Pathways allocation PHY23034. M.G. was supported by BSF grant 2024801. This work was partially supported by the International Space Science Institute (ISSI) in Bern through International Team project no. 23-575.

Declaration of interests

The authors report no conflict of interest.

REFERENCES

AGAPITOV, O.V., KRASNOSELSKIKH, V., BALIKHIN, M., BONNELL, J.W., MOZER, F.S. & AVANOV, L. 2023 Energy repartition and entropy generation across the Earth's bow shock: MMS observations. *Astrophys. J.* **952**, 154.

BOWERS, K.J., ALBRIGHT, B.J., YIN, L., BERGEN, B. & KWAN, T.J.T. 2008 Ultrahigh performance three-dimensional electromagnetic relativistic kinetic plasma simulation. *Phys. Plasmas* **15**, 055703.

DE HOFFMANN, F. & TELLER, E. 1950 Magneto-hydrodynamic shocks. *Phys. Rev.* **80**, 692–703.

DU, S., ZANK, G.P., LI, X. & GUO, F. 2020 Energy dissipation and entropy in collisionless plasma. *Phys. Rev. E* **101**, 033208.

LANDAU, L.D. & LIFSHITZ, E.M. 1987 Fluid mechanics. In *Course of Theoretical Physics*, 2nd edn, vol. 6. Pergamon Press.

LANDAU, L.D., LIFSHITZ, E.M. & PITAEVSKIĬ, L.P. 1984 *Electrodynamics of Continuous Media*, 2nd edn, vol. 8. Pergamon Press.

LIANG, H. *et al.* 2019 Decomposition of plasma kinetic entropy into position and velocity space and the use of kinetic entropy in particle-in-cell simulations. *Phys. Plasmas* **26**, 082903.

MOUHOT, C. & VILLANI, C. 2011 On Landau damping. *Acta Mathematica* **207**, 29–201.

PARKS, G.K. *et al.* 2012 Entropy generation across Earth's collisionless bow shock. *Phys. Rev. Lett.* **108**, 061102.

REICHL, L. 2009 *A Modern Course in Statistical Physics*. Wiley.

SARAZIN, Y., DIF-PRADALIER, G., ZARZOSO, D., GARBET, X., GHENDRIH, P. & GRANDGIRARD, V. 2009 Entropy production and collisionless fluid closure. *Plasma Phys. Control. Fusion* **51**, 115003.

SCHWARTZ, S.J. *et al.* 2022 Energy partition at collisionless supercritical quasi-perpendicular shocks. *J. Geophys. Res.* **127**, e2022JA030637.

https://doi.org/10.1017/S002237782610172X Published online by Cambridge University Press